



CHARACTERIZATION AND MODELING OF SOME PHYSICAL AND CHEMICAL PARAMETERS OF TWO ACTIVATED CARBONS SYNTHESIZED UNDER OPTIMAL CONDITIONS FROM 2^k FULL FACTORIAL DESIGN

YAO Marcel Konan¹, GOULI Bi Irié Marc¹, AKPETOU Kouamé Lazare², N'ZUÉ Yao Gaston¹, BLÉ Melecony Célestin³, TROKOUREY Albert¹

¹Physic chemistry Laboratory, University Félix Houphouët-Boigny of Cocody Abidjan, UFR SSMT, 22 B.P. 582 Abidjan 22, Abidjan, Côte d'Ivoire.

²UP Chemistry and Physic, University Jean Lorougnon Guédé, Daloa, Côte d'Ivoire.

³Océanologic Research Center of Abidjan, Rue des pêcheurs, BP V 18 Abidjan, Cote d'Ivoire.

ABSTRACT

The upgrading of wastes for use in environmental remediation is a major challenge for developing countries, such as Côte d'Ivoire. It is in this context that kernel shells of *Elaeis guineensis* drupe and kernels of *Dacryodes klaineana* fruit were used for synthesis of activated carbons. 2^k full factor design was implemented to obtain activated carbons having a maximum of mini and average micropores respectively with these two lignocellulosic materials. The results obtained show that kernel shells of *Elaeis guineensis* drupe, having a sharpness to form more activated carbons having a maximum of mini micropores. On the other hand, kernels of *Dacryodes klaineana* fruit makes it possible to obtain activated carbons of high capacity having a maximum of average micropores under defined experimental conditions. The use of normed principal components analysis and Spearman's non-parametric coefficient showed strong direct and/or indirect correlations between all physical and chemical parameters evaluated on these carbons, including factors for their preparation. In addition, the use of simple linear regression allowed more than 80% prediction of some of these parameters from the activation temperature in most cases.

KEY WORDS: Agricultural waste, Côte d'Ivoire, *Dacryodes klaineana*, *Elaeis guineensis*, Modeling.

INTRODUCTION

Côte d'Ivoire is subject to anarchic urbanization under the pressure of an annual 1.88% growth rate (World Bank, 2017). That results of an estimated population of 23,740,424 in habitants overwhelmed by informal workers in the towns who mainly leave the rural areas. There, a rain-forest based agriculture is no more possible due to deforestation (GIZ, 2013). Therefore, people migrate in towns because of the upgrading challenge the traditional agriculture face yearly due to the effects of climate change.

Several ecological problems originate from the implementation of these informal activities. And, managing the development and intensification of those anthropogenic activities is a huge challenge for municipalities and the governments. Pollutants are directly released into the environment without prior treatment. This situation leads to the pollution of the ivorian ecosystem in general (air (N'Gotta, 2009), soils (Guety et al., 2015) and waters (N'guessan et al., 2015)). Globally, since there are no real networks for sewage treatments and waste collections in cities like Abidjan district (Gnagne, 2015).

Research activities aimed to face this concern for years. And the development of ecological technologies such as activated carbon for wastes treatment is carried out in recent works (Bamba et al., 2009; Ello et al., 2013;

Gnonsoro et al., 2015; Kouakou et al., 2017, etc.). To countries like Côte d'Ivoire, the sources of carbon are an advantage. Thus, known by the trivial name of "oil palm", *Elaeis guineensis* (or *Elaeis guineensis* Jacq.) is widely grown for its fruits and seeds which are rich in oil for food and industry use. The residual kernel shells, commonly rejected in the environment, were shown to be a precursor in the manufacture of a cost-effective activated carbons of good qualities (Ello et al., 2013; Okoroigwe et al., 2013; Olowoyo and Orere, 2012). That drove the works of some authors like Ruiz et al. (2015), Yuliusman et al. (2017) and Wahyuningsih et al. (2018). This study aimed to increase the knowledge about the conditions of making high quality activated carbons. To do so, kernels of two vegetable detritus namely *Elaeis guineensis* and *Dacryodes klaineana* were used.

Activated carbons are generally obtained in two modes: physical activation and chemical activation. However, the chemical activation is cheap, less tedious (achieved in one step), facilitates control of the pore size distribution and limits the burn-off; although carbons prepared present impurities on their surface (Chauvin, 2015). These reasons justified the choice of this method for the synthesis of our carbons from these two precursors mentioned above. Optimization of the results of chemically activated carbons depends on some factors in which the most influential are the activation agent, the impregnation rate, the activation

temperature and the activation time. These factors determine properties of activated carbons in terms of pore volume, pore size distribution and chemical composition of the surface (Chauvin 2015, Meljac 2014). The simultaneous control of these factors for obtaining optimal activated carbons according to experimental conditions is not easy (Meljac, 2004). The experimental research methodology is often used for such purposes. One of experimental designs showing good acuity in this area is 2^k full factorial design, as illustrated by several studies (Gueye *et al.*, 2011; Kouotou *et al.*, 2013; Marouane *et al.*, 2016; Nwabanne and Igbokwe, 2011). Thus, it is a major interest for this study to:

- the synthesis under optimal conditions of activated carbons based on kernel shells of *Elaeis guineensis* drupe and kernels of *Dacryodes klaineana* fruit by the use of 2^k full factorial design, namely the search for factors among those initially set to obtain activated carbons having a maximum of mini micropores and average micropores;
- the physical and chemical characterizations of these carbons;
- the modeling of some physical and chemical characteristics of these carbons from others such as some factors used for their synthesis and/or another

physical and chemical characteristics are relatively easy to get.

MATERIALS & METHODS

Experiments planification by 2^k full factorial design

The activation agent, the impregnation rate, the activation time and the activation temperature were considered as factors in this study. Taking into account their acid-base characteristics and their capacity in the development of activated carbons, 3 activation agents were chosen in this study. These are H_3PO_4 (30%), $ZnCl_2$ (1N) and KOH (1N). the impregnation rate was considered for two threshold values, 1 and 3. Referring to the scientific literature and the lignocellulosic composition of our precursors, the activation time was set at 30 min and 45 min. For these same reasons, the activation temperature was set at 800°C and 900°C for kernel shells of *Elaeis guineensis* drupe, and at 300°C and 400°C for kernels of *Dacryodes klaineana* fruit. The use of 3 activation agents in this study leads to the definition of 3 experimental domains for each precursor, given in Table 1. The responses considered in this study are iodine and methylene blue numbers. Iodine number was used for the of the mini micropores importance and, methylene blue number for that of the average micropores in activated carbons obtained according to established experimental designs.

Table 1: Experimental domains for activated carbons synthesis based on kernel shells of *Elaeis guineensis* drupe and kernels of *Dacryodes klaineana* fruit.

Experimental domains	Variables	Factors	Kernels shells of <i>Elaeis guineensis</i> drupe		Kernels of <i>Dacryodes klaineana</i> fruit	
			Level		Level	
			-1	+1	-1	+1
1	X_1	Impregnation rate	1	3	1	3
	X_2	Activation agent	H_3PO_4 (30%)	$ZnCl_2$ 1N	H_3PO_4 (30%)	$ZnCl_2$ 1N
	X_3	Activation time	30 mn	45 mn	30 mn	45 mn
	X_4	Activation Temperature	800°C	900°C	300°C	400°C
2	X_1	Impregnation rate	1	3	1	3
	X_2	Activation agent	H_3PO_4 (30%)	KOH 1N	H_3PO_4 (30%)	KOH 1N
	X_3	Activation time	30 mn	45 mn	30 mn	45 mn
	X_4	Activation temperature	800°C	900°C	300°C	400°C
3	X_1	Impregnation rate	1	3	1	3
	X_2	Activation agent	$ZnCl_2$	KOH 1N	H_3PO_4 (30%)	KOH 1N
	X_3	Activation time	30 mn	45 mn	30 mn	45 mn
	X_4	Activation temperature	800°C	900°C	300°C	400°C

Protocols used for activated carbons synthesis and for their physical and chemical characterizations

Activated carbons synthesis

The raw materials, namely kernel shells of *Elaeis guineensis* drupe and kernels of *Dacryodes klaineana* fruit, were recovered in detritus. Previously, they were washed several times and then dried. The kernel shells of *Elaeis guineensis* drupe were later crushed in small variable sizes. These kernel shells and kernels of *Dacryodes klaineana* fruit were pickled to remove fine and pulp residues respectively. These entities were further

washed and then oven-dried at 105°C for 24 H. These precursors were then impregnated for 24 H in various activation agents according to the impregnation rate pre-established in different experimental designs. They were then pyrolyzed and activated in a muffle furnace in accordance with conditions established by these designs. Activated carbons obtained are treated according to the activating agent used. Those obtained by impregnation with $ZnCl_2$ (1N) are abundantly washed with demineralised water. The rinse water is each time controlled by adding a solution of 0.1M $AgNO_3$, to ensure

the maximum elimination of this activating agent. For carbons from the impregnation of KOH (1N) and H₃PO₄ (30%), they are thoroughly rinsed with deionized water until pH of the rinsing water is close to neutral. All these carbons are dried oven-dried at 105°C after this step for 24 H.

Physical and chemical characterizations

Yield, moisture, ash, bulk density

Determining the percentage by mass of carbon in activated carbons, the yield (R) is given as follows:

$$R = \frac{m_2}{m_1} \times 100 \quad (1)$$

with, m₁ the mass of the precursor used for the activated carbon synthesis and m₂ the mass of the activated carbon obtained from the mass m₁ of the precursor.

The moisture of activated carbons was determined in accordance with ASTM D 2867-09 (2014). It consists of carrying in the oven-dried during 24 H and at 105°C, a porcelain crucible, weighed initially, containing 2 g of activated carbon. After having removed it from the oven-dried and allowed to cool to the desiccator, the crucible is weighed again. The moisture of the sample is obtained according to the formula below.

$$\text{Moisture (\%)} = \frac{m_4 - m_5}{m_4 - m_3} \quad (2)$$

with m₃ the initial mass of the activated carbon (2 g), m₄ the mass of the crucible + 2 g of the activated carbon before passing to the oven-dried and m₅ the mass of the crucible + 2 g of the activated carbon after passing to the oven-dried.

The ash of activated carbons was evaluated according to ASTM D3174-73 (2012). A sample of 1 or 2 g, screened between 0.15 and 0.25 mm, was dried in an oven-dried for 12 H and then placed in a previously weighed porcelain capsule. This capsule was introduced into an oven-dried and heated for 30 min at 773K (500°C) and then for 4 H up to 1085K (812°C). Once incineration is complete, the oven-dried is allowed to cool and the capsule is recovered and weighed. In a similar way to the moisture, the ash of the activated carbon was determined according to formula 2. The bulk density of activated carbons was determined in accordance with ASTM D2854-09 (2014). A sample of the activated carbon was carried in a volumetric flask, previously weighed empty, up to the mark. This flask is

then reweighed. The bulk density of the activated carbon is determined as follows:

$$\text{Bulk density} = \frac{m_7 - m_6}{V} \quad (3)$$

with, m₆ the mass of the empty flask, (in g (kg)), m₇ the mass of the flask containing the activated carbon up to the mark (in g (kg)), v the volume of the flask (in cm³ (m³)) and the bulk density (in g/cm³ (Kg/m³)).

pH, zero charge pH (pH_{ZC}) and Conductivity

pH of activated carbons was determined according to ASTM D 3388-80 (1999). It consists in shaking for 24 H, a solution containing 2g/L of the activated carbon. In the following, the mixture is filtered on a Whatman type filter paper. pH of the activated carbon corresponds to that of the filtered solution. Correlatively, the conductivity of these carbons has been measured under these same conditions.

Regarding zero charge pH (pH_{ZC}), it was determined by the NaCl method as described by Lopez-Ramon et al. (1999). For this purpose, 0.1 g of the activated carbon was brought into contact with 20 ml of 0.1 M NaCl solutions and with pH of between 2 and 10 (adjusted by addition of an aqueous solution of NaOH or HCl) in tightly closed flasks. The suspensions were stirred for 3 days at room temperature. Each solution was then filtered on Whatman type paper and pH of the filtered solution was measured. From the plot curve final pH = f (initial pH), pH_{ZC} of the activated carbon was determined as pH of the solution for which the curve crosses the first bisector (final pH = initial pH).

Iodine and methylene numbers

The iodine number of activated carbons was determined using the experimental protocol proposed by ASTM D4607-94 (2011). 1 g of dry activated carbon was contacted with 10 ml of 5% HCl solution in 250 ml of a clean dry Erlenmeyer flask. The whole was stirred and brought to a gentle boil for about 30 s. 100 ml of a standard solution of 0.1N iodine is introduced into the mixture. Immediately the flask was sealed again and stirred for 30 s. In the following, it is filtered quickly. A volume of 50 ml of the filtrate was taken and titrated with a solution of 0.1N Na₂S₂O₈ in the presence of starch paste. The iodine number of the activated carbon is obtained by first estimating the amount of iodine absorbed in meq (X').

$$X \text{ (meq)} = 100 \times N_1 - \frac{100 \times N_2 \times V}{50} \quad (4)$$

with N₁ the normality of the iodine solution (0.1 N), N₂ the normality of Na₂S₂O₈ solution (0.1 N), V the volume of Na₂S₂O₈ used for the assay.

The iodine number relative to the mass of the carbon (g) is given by:

$$\text{Iodine number (mg/g)} = \frac{X}{m} \times A \quad (5)$$

with A the correction factor obtained after calculating the normality of the residual filtrate, X the amount of iodine absorbed in mg and obtained as follows:

$$X = 126,93 \times X \quad (6)$$

The methylene blue number is defined as the maximum level of methylene blue absorbed by 1g of activated carbon (Nunes and Guerreiro, 2011). This parameter was obtained according to ECCMF (1986) in this study. The determination of the methylene Blue number by this method was done in 2 steps. The first step consisted in the preparation of 1.2 g/L methylene blue solution, which was

left standing for 24 H in the dark. The title of this solution is tested the next day by adding 0.25% CH₃COOH (5 ml per 1L of solution) and performing a UV spectrophotometric reading at 620 nm on a 1 cm layer. The result of the absorbance should be 0.840 ± 0.01 nm. If the absorption is too high, the required amount must be corrected after calculation with distilled water. If it is too

weak, the solution must be prepared again. The second step properly concerned the methylene blue test. It consisted in stirring a mixture consisting of 0.1g of activated carbon with 5 ml of the prepared methylene blue solution until the solution became discolored. The operation was resumed by adding 5 ml of the methylene blue solution and repeated several times for 5 min. It is

$$\text{Methylene blue number (mg/g)} = \frac{(C_i - C) \times V \times M_{\text{BM}}}{m} \quad (7)$$

with, C_i and C_e initial and residual concentration of methylene blue (mol/L) respectively, V the total volume of the methylene blue solution used (L), m mass of the activated carbon used (in this case 0.1 g), M_{BM} molar mass of methylene blue (319.85 g/mol).

Surface areas obtained according acetic acid and methylene blue adsorption methods

The characterization of the surface occupied by mini micropores in activated carbons was doing by the acetic acid absorption method, as developed by Avon *et al.* (2000). 1 g of activated carbon was added to 50 ml of

$$Q \text{ (mol/g)} = \frac{(C_i - C) \times V}{m} \quad (8)$$

with, C_i and C_e initial and residual concentration of acetic acid (mol/L), V the volume of acetic acid in each Erlenmeyer flask ($V = 50$ ml).

The determination of the surface area is doing from the Langmuir equation, used as follows:

$$\frac{C}{Q} = \frac{C_e}{Q_m} + \frac{1}{Q_m \times k} \quad (9)$$

Q_m , the maximum amount of acetic acid absorbed (in mol/g) is deduced from the slope of $\frac{C}{Q_e} = f(C_e)$. The knowledge of this parameter leads to the determination of the surface area of the activated carbon bound to acetic acid ($S_{\text{acetic acid}}$) by the equation:

$$S_{\text{acetic acid}} = Q_m \times S \quad (10)$$

with, $S = 21 \text{ \AA}$ the area occupied by a acetic acid molecule (Shoemaker *et al.*, 1981); the Avogadro number (6.022×10^{23}).

The methylene blue adsorption method was used to assessment the surface area due to average micropores of activated carbons. It has the same principle and calculation methods as the acetic acid adsorption method for the surface area determination, but differs in the area S occupied by the methylene blue molecule ($S = 175 \text{ \AA}$

noted the total volume V of methylene blue solution during these 5 min. The amount of methylene blue remaining is obtained by UV spectroscopic assay at 665 nm compared to a previously established calibration curve. The methylene blue number of the activated carbon is given by:

acetic acid solutions of different initial concentrations (0.015, 0.025, 0.1 and 0.15 mol/L) in Erlenmeyer flasks. These Erlenmeyer flasks were then hermetically sealed and stirred regularly for 1 H at room temperature. After this operation, the mixtures were filtered on Whatman type filter paper. 10 ml of the filtrate were collected and then assayed with 0.1 M NaOH solution for the determination of the equilibrium concentration (C_e) of acetic acid. The amount of acetic acid adsorbed at equilibrium (Q_e) is given by:

(Nunes and Guerreiro, 2011)). In this study, 10g (m) of activated carbon were contacted with a certain volume V of methylene blue at various concentrations (10, 25, 50, 100, 250, 500 and 1000 mg.L⁻¹). The whole was stirred for 24 H. After filtration on Whatman type filter paper, the residual concentration of methylene blue was determined by UV spectroscopy at 620 nm. Concentrations used being in mg/L, equations (8) and (10) become:

$$Q_e \text{ (mg/g)} = \frac{(C_i - C_e) \times V \times M_{\text{BM}}}{m} \quad (11)$$

$$S_{\text{methylene blue}} = \frac{Q_m \times S \times \text{\AA}}{M_{\text{BM}}} \quad (12)$$

with, C_i and C_e initial and residual concentration of methylene blue (mol/L) respectively, V the total volume of the methylene blue solution used (L), m mass of the activated carbon used (in this case 0.1 g), M_{BM} molar mass of methylene blue (319.85 g/mol).

Surface functions

The dosage of acidic and basic surface functions was done according to the Boehm method (1966). It consisted of bringing into contact 0.2 g of activated carbon (previously dried at 105°C in an oven-dried for 24 H) with 50 ml of a

0.1N solution of one of the following four bases: NaHCO₃, Na₂CO₃, NaOH, NaOC₂H₅. The mixture was stirred for 48 H. After stirring, the suspension was filtered through Whatman filter paper. The excess of basic solution was measured in return by 0.1N HCl solution. The assay of chromene and pyrone (basic surface functions) was carried out from 0.2 g of activated carbon reacted by stirring for 48 H with 50 ml of 0.1N HCl. After filtration of suspension through Whatman filter paper, the excess acid was assayed back with 0.1N NaOH solution. These acid-

base assays were performed by titrimetry. The number of gram equivalents of each chemical compound used having

$$\text{neqR} = N_i V_i - N_f V_f \quad (13)$$

with, neqR the number of equilibrium gram having reacted; $N_i V_i$ and $N_f V_f$ the number of gram equivalents before and after reaction.

The use of NaHCO_3 makes it possible to highlight carboxylic functions on activated carbons. That of Na_2CO_3 does it possible to identify simultaneously carboxylic functions and lactone functions on these entities. The application of NaOH makes it possible to characterize all the carboxylic, lactones and phenolic functions. Carbonyl functions are highlighted by $\text{C}_2\text{H}_5\text{ONa}$ (Maazou *et al.*, 2017). Thus, is it deduced the number of gram equivalent of each function present on the surface of the carbon by appropriate differences.

Primary polar sites number (a_0), saturating water capacity (a_s) and interfacial tension (σ_0)

For activated carbons, oxygen functions are chemically bonded to the surface of the material. Heteroatoms also constitute polar sites during activation (Baudu *et al.*, 2001), which contribute to the hydrophobic or hydrophilic nature of activated carbons, and are primary polar sites likely to be occupied by small polar molecules, particularly water. The determination of primary polar

reacts with the amount of activated carbon used is given by:

sites number likely to be occupied by small polar molecules (a_0), the maximum water adsorption capacity (a_s) and the hydrophilic character (σ_0) of activated carbons was done by the isothermal method of water vapor and the spreading pressure as recommended by Baudu *et al.* (2001).

It consisted of putting known masses of activated carbons, previously dried in an oven-dried at 105°C for 72 H, in saturated aqueous salt solutions whose water vapor pressures were known. These solutions were subsequently placed in desiccators for 192 H. After this equilibrium time, the quantity of water adsorbed on activated carbons at P/P_0 (partial pressure) was evaluated by weighing. The exploitation of the water vapor adsorption isotherm, according to a localized adsorption model of Langmuir, then leads to the global estimation of hydrophilic sites linked to both acidic and mineral area functions (a_0). This capacity is compared with the saturation capacity (partial water pressure = 1) a_s . The determination of the parameter a_0 is carried out by plotting the function $(P/P_0)/a = f(P/P_0)$ from the following equation:

$$a = \frac{a_0 \times K \times (P/P_0)}{1 - K \times (P/P_0)} \quad (14)$$

The interfacial tension σ_0 is obtained by the integration of the Gibbs equation (Julien *et al.*, 1998) defined as follows:

$$\sigma_0 = \frac{RT}{S} \times \int_0^1 \frac{a}{(P/P_0)} d(P/P_0) \quad (15)$$

Where, K = constant; a = the amount of water adsorbed onto the activated carbon (mmol.g^{-1}) at P/P_0 ,

P/P_0 = partial pressure (in $1.013 \cdot 10^5$ Pa), σ_0 = interfacial tension (mJ.m^{-2}), R = constant of perfect gases ($8.314 \text{ J.K}^{-1} \cdot \text{mol}^{-1}$); T = absolute temperature ($293 \text{ }^\circ\text{K}$) and S = Surface area ($\text{m}^2 \cdot \text{g}^{-1}$).

The chemical compounds used in this context are given in Table 2. An extrapolation was doing in this study by calculating σ_0 with $S_{\text{methylene blue}}$ to better estimate the character of activated carbons synthesized with respect to big molecules, particularly of the methylene blue size.

TABLE 2: Relatively humidity of chemical compounds used for the realization of the isothermal method of water vapor and the spreading pressure in this study

Chemical compounds	P/P0 (bars) at 25°C
KOH	8
NaCl	75
NH_4Cl	78,57
MgSO_4	88,6
Na_2CO_3	92
K_2SO_4	97

Modeling of some physical and chemical parameters of activated carbons

Modeling of some physical and chemical parameters of activated carbons was based on their prediction on the basis of other parameters such as initial factors involved in their preparation and/or those whose obtaining is relatively easy. The first phase was a correlative approach to better identify parameters that can be easily modeled by simple regressions. For this purpose, it used normed principal

components analysis (NPCA) and Spearman's non-parametric correlation coefficient (r'). NPCA was performed considering significant correlations at $p < 0.5$, and r' was performed at 5% confidence interval according to the student test. The second phase consisted in modeling using simple linear regression. All these statistical calculations were doing using Statistical version 10.0 software.

RESULTS & DISCUSSION**Optimum conditions for activated carbons synthesis according to objectives set****Activated carbons based on kernel shells of *Elaeis guineensis* drupe (CAPH)**

The results presented in Table 3 (experiment 21) and in fig. 1A clearly show that ZnCl₂ is the best activation agent leading to obtaining CAPH having a maximum of mini micropores in this study. In general, ZnCl₂ (1N) increases the iodine adsorption of 295.78 mg/g, unlike H₃PO₄ (30%) and KOH (1 N) which do that of 150.26 mg/g and 196.48 mg/g respectively. H₃PO₄ and ZnCl₂, are known for their ability to form activated carbons with a significant number of micropores with lignocellulosics (Bamba *et al.*, 2009; Sethupathi *et al.*, 2015). However, high activation temperatures used in this context would inhibit the action of H₃PO₄, but favor that of ZnCl₂. Indeed, for temperatures below 450°C, H₃PO₄ leads to a contraction of the carbon structure following the formation of phosphate bonds between graphenes. On the other hand, for those higher

than 450°C, these bonds become unstable and lead to the collapse of pores, while regenerating H₃PO₄ molecules (Cao *et al.*, 2018; Chauvin, 2015). For KOH, these high activation temperatures cause the destruction of mini micropores due to strong collisions of potassium ions (K⁺) with the surface of carbons formed (Andas *et al.*, 2017). Also, high concentrations of H₃PO₄ and KOH used in this study contributed to this process. For ZnCl₂, its melting temperature of 580°C, would explain its ability to form mini micropores on carbons above 800°C (Chauvin, 2015; Xia *et al.*, 2018), particularly with this precursor as noted by Hidayua and Mudaa (2016). The increasing of the activation temperature, from 800°C to 900°C, promotes the iodine adsorption of 45.02 mg/g. It is the same case for the increase of activation time, from 30 min to 45 min, which increases this adsorption of 44.70 mg/g. On the other hand, the increase of the impregnation rate, from 1 to 3, reduces this adsorption of 38.58 mg/g. This established fact is classic in the development of activated carbons (Chauvin, 2015).

TABLE 3: Synthesis of the implementation of 3 experiment designs with iodine and methylene blue numbers as responses

Experience	Factors				CAPH		CAF		
	X1	X2	X3	X4		Q _{I2} (mg/g)	Q _{BM} (mg/g)	Q _{I2} (mg/g)	Q _{BM} (mg/g)
				CAPH	CAF				
1	1	H ₃ PO ₄ (30%)	30 min	800°C	300°C	51.21	0.39	66.62	-
2	3	H ₃ PO ₄ (30%)	30 min	800°C	300°C	260.04	4.81	64.54	-
3	1	ZnCl ₂ (1N)	30 min	800°C	300°C	340.76	-	19.86	-
4	3	ZnCl ₂ (1N)	30 min	800°C	300°C	432.81	-	40.84	900.21
5	1	KOH (1N)	30 min	800°C	300°C	262.53	-	7.48	-
6	3	KOH (1N)	30 min	800°C	300°C	241.90	1.88	8.47	153.45
7	1	H ₃ PO ₄ (30%)	45 min	800°C	300°C	195.70	60.49	6.38	-
8	3	H ₃ PO ₄ (30%)	45 min	800°C	300°C	170.21	166.67	24.28	-
9	1	ZnCl ₂ (1N)	45 min	800°C	300°C	320.28	-	31.93	-
10	3	ZnCl ₂ (1N)	45 min	800°C	300°C	179.12	-	31.87	-
11	1	KOH (1N)	45 min	800°C	300°C	169.21	-	38.99	1161.41
12	3	KOH (1N)	45 min	800°C	300°C	183.12	-	36.60	1331.50
13	1	H ₃ PO ₄ (30%)	30 min	900°C	400°C	249.49	4.54	25.01	-
14	3	H ₃ PO ₄ (30%)	30 min	900°C	400°C	147.29	0.49	8.45	-
15	1	ZnCl ₂ (1N)	30 min	900°C	400°C	232.04	-	6.99	-
16	3	ZnCl ₂ (1N)	30 min	900°C	400°C	275.91	-	19.64	-
17	1	KOH (1N)	30 min	900°C	400°C	238.29	38.45	22.31	-
18	3	KOH (1N)	30 min	900°C	400°C	201.72	655.20	19.87	1343.96
19	1	H ₃ PO ₄ (30%)	45 min	900°C	400°C	214.49	185.68	7.20	709.77
20	3	H ₃ PO ₄ (30%)	45 min	900°C	400°C	178.61	296.69	7.77	-
21	1	ZnCl ₂ (1N)	45 min	900°C	400°C	890.16	-	11.26	-
22	3	ZnCl ₂ (1N)	45 min	900°C	400°C	216.83	-	30.80	-
23	1	KOH (1N)	45 min	900°C	400°C	255.08	-	12.56	-
24	3	KOH (1N)	45 min	900°C	400°C	366.59	11.21	10.40	1479.98

- CAPH, activated carbon based on kernel shells of *Elaeis guineensis* drupe;

- CAF, activated carbon based on kernels of *Dacryodes klaineana* fruit;

- Q_{I2}, quantity of iodine adsorbed,

- Q_{BM}, quantity of methylene blue adsorbed.

KOH represents the best activation agent for obtaining CAPH containing a high number of average micropores under experimental conditions used (experiment 18 (Table 3) and Fig. 1B). KOH (1N) increases the blue methylene adsorption at 358.38 mg/g while H₃PO₄ (30%) do it at 179.94 mg/g and ZnCl₂ (1N) very weakly at 0.2 mg/g. This result confirms the good ability of KOH to form activated carbons having a great number of average

micropores with high lignocellulosic content materials, as mentioned by Ruiz *et al.* (2015) and Shen *et al.* (2018). This phenomenon is favored by a superficial attack of lignite and cellulose by KOH after its carbonation in KHCO₃ then in K₂CO₃ (Andas *et al.*, 2017; Chauvin, 2015), but also by a vigorous attack on the surface of these carbons by potassium ions (K⁺) for these high temperatures (Andas *et al.*, 2017). The increase of the

impregnation rate, from 1 to 3, contributes to the optimal formation of these micropores, as illustrated by the increase of the methylene blue adsorption of 197.76 mg/g. This classic fact is explained by the nature and texture of kernel shells of this substrate, which is a compound with a high lignocellulosic composition (29.7% of cellulose, 53.4% of lignin and 47.7% hemicellulose/ halocellulose) (Chauvin 2015; Setethupathi *et al.*, 2015). These same remarks were noted with this same precursor by Andas *et al.* (2017), Ello *et al.* (2013) and Yuliusman *et al.* (2017). The increase of the activation temperature, from 800°C to 900°C, promotes this process, by increasing the blue methylene adsorption of 45.02 mg/g. However, the increasing of the activation time, from 30 min to 45 min, generally contributes to the decrease of the methylene blue adsorption of 118.76 mg/g.

Activated carbons based on kernels of *Dacryodes klaineana* fruit (CAF)

The nature and texture of kernels of *Dacryodes klaineana* fruit would lead to the observation of a competition between oxidants used to obtain CAF having a maximum of mini micropores. This situation is illustrated by a small difference observed between responses of these oxidants on all experiments carried out (Fig. 1C), with a slight advantage for H₃PO₄. This is also shown by the relative highest iodine adsorption obtained in experiment 1 (Table 3). For illustration, H₃PO₄ (30%) increases the iodine adsorption of 452.56 mg/g compared to that of ZnCl₂ (1N) and KOH (1N), which do that of 448.3 mg/g and 439.16 mg/g. This clear difference of H₃PO₄ with respect to the other two oxidants, particularly ZnCl₂, would be due to activation temperatures used. Indeed, for activation temperatures of the order of 300°C to 400°C, the formation of mini micropores from lignocellulosic materials with H₃PO₄ would be due to the development of pore shaped bottles because of stability phosphate bonds (Cao *et al.*, 2018; Chauvin, 2015). This observation is in agreement with those of Maazou *et al.* (2017) and Ousmaila *et al.* (2016), who noted that H₃PO₄ delays thermal decomposition while limiting volatile losses and leading to the formation of a rigid carbon matrix. For ZnCl₂, this temperature range used in this context corresponds to which its influence on the thermal decomposition of lignin begins to be significant (Chauvin, 2015). So, its action would be partial at these temperatures. Moreover, the strong oxidizing character of KOH, H₃PO₄ and ZnCl₂ would result in the destruction of mini micropores with this type of low cellulosic material that the nature and composition is very close to that of *Dacryodes edulis* (Ebana *et al.*, 2017). The formation of mini micropores with this precursor is generally disadvantaged by the increase of the activation temperature (from 300°C to 400°C) and the activation time (from 30 min to 45 min), which decrease the iodine adsorption of 32.60 mg/g and 10 mg/g respectively. However, the impregnation rate promotes it to 7.82 mg/g. In this case also, KOH leads to the production of an activated carbon based on this precursor with a relative maximum of average micropores. This fact is illustrated by the results obtained in the experiment 24 (Table 3) and in fig. 1D. KOH (1N) increases highly methylene the blue adsorption at 2155.8 mg/g, and ZnCl₂ (1N) and H₃PO₄ (30%) do it at 1800.21 mg/g and 1419.54 mg/g

respectively. Thus, KOH would achieve a good migration and carbonation on fibers of these precursors. Therefore, the capacity of KOH formed this type of pores with materials with low lignocellulosic contents has just been confirmed once again, as noted by Elmouwahidi *et al.* (2017) and González-García (2018). H₃PO₄ and ZnCl₂, by their strong oxidizing character higher than KOH (Chauvin, 2015) and their high concentrations used in this context, would lead more to the collapse of pores formed with precursor. The increases of the activation time (from 30 min to 45 min), the activation temperature (from 300°C to 400°C) and the impregnation rate (from 1 to 3), generally favors the formation of average micropores, shown by the increase of the blue methylene adsorption at 212.46 mg/g, 757.40 mg/g and 582.52 mg/g respectively.

Physical and chemical characteristics of synthesized activated carbons

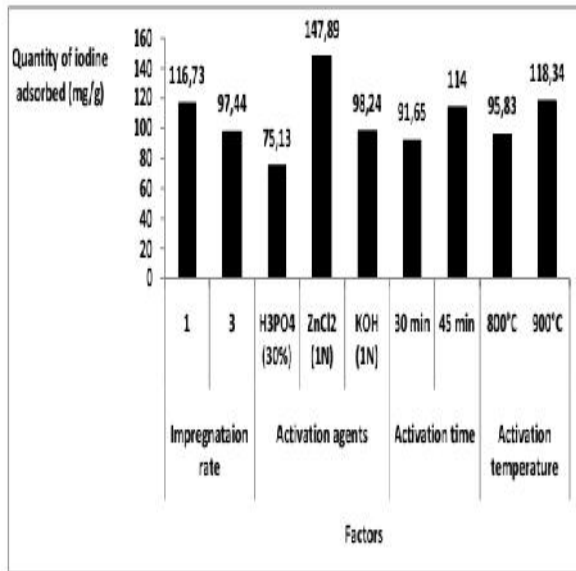
In the following, the activated carbon obtained from kernel shells of *Elaeis guineensis* drupe and having a maximum of mini micropores in this study is designated CAPH1. That resulting from this same precursor and having a maximum of average micropores is denoted by CAPH2. It is the same for activated carbons based on kernels of *Dacryodes klaineana* fruit, which for the one containing a maximum of mini micropores is designated CAF1 and the other having a maximum of average micropores by CAF2. The different characteristics of activated carbons obtained are given in the table 4.

There is a relatively important difference between yields of activated carbons obtained from kernel shells of *Elaeis guineensis* drupe and those from kernels of *Dacryodes klaineana* fruit. This is also the case between activated carbons from the same precursor, particularly for kernels of *Dacryodes klaineana* fruit where this fact is important. These observations are consecutive to the difference of activation temperatures and activation times of these carbons. Indeed, under the effect of an increase in heat with/or that of the activation time, the loss of macromolecules is important (Andas *et al.*, 2017; Maazou *et al.*, 2017; Wahyuningsih *et al.*, 2018). All carbons have a low ash. This fact reflects the good carbonization of the precursors in the temperature range used, leading to the devolatilization of the lignin of these carbonaceous biomasses. These results confirm the composition of precursors used mainly by organic matter, particularly carbon (Ebana *et al.*, 2017; Setethupathi *et al.*, 2015). Carbons obtained by treatment with KOH (CAPH2 and CAF2) have the highest ash. This finding would suggest that the decomposition of hemicellulose and cellulose by KOH is relatively less important than that achieved by H₃PO₄ and ZnCl₂. Therefore CAPH2 and CAF2 contain more impurities than CAPH1 and CAF1. This would reduce their ability to purify aqueous solutions compared to other two carbons (Okoroigwe *et al.*, 2013). These ash values show that all synthesized carbons have significant activity and relatively high reactivation potential (Olowoyo and Orere, 2012). Like their ash, the moisture of these carbons is low. This would indicate their superior quality and promote adsorption (Zeroual *et al.*, 2011). Again, it illustrate their high calorific value (Mbaye, 2014), especially when kernels of *Dacryodes klaineana* fruit is treated with H₃PO₄. The bulk density of these different activated carbons are all in the standard range

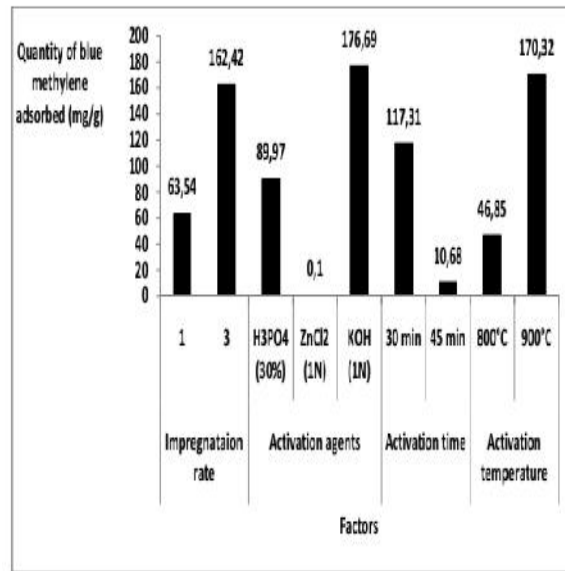
Optimal synthesis of two activated carbon

(240 to 780 Kg/ m³ (Okoroigwe *et al.*, 2013)). These carbons would therefore have a highest volume of activity and present an optimal quality. These characteristics

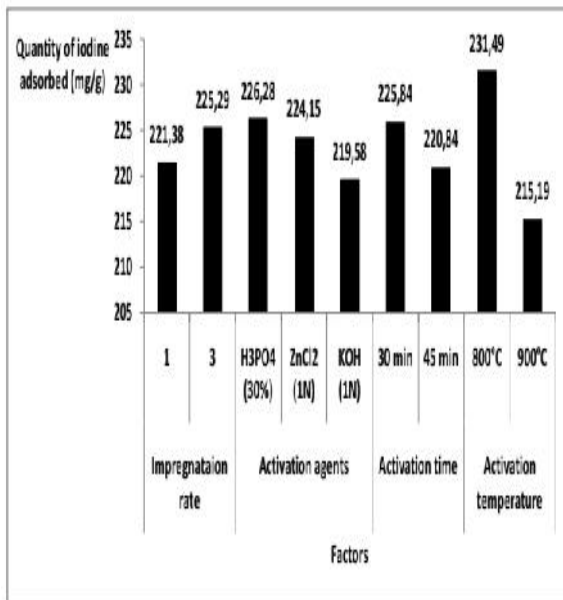
would show the good quality of these two precursors for the production of activated carbons.



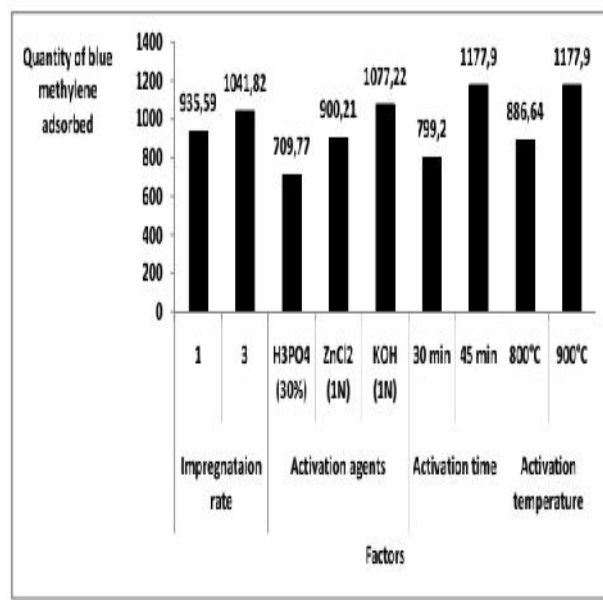
A



B



C



D

FIGURE 1: Mean effects of main factors on responses for CAPH (iodine (A) and methylene blue (B) adsorptions) and CAF (iodine (C) and methylene blue (D) adsorptions).

TABLE 4: Some physical and chemical characteristics of activated carbons synthesized

Physical and chemical parameters		CAPH1	CAPH2	CAF1	CAF2
	Texture	grain	grain	powder	powder
	Yield (%)	26.00	22.51	65.63	45.37
	Ash (%)	1.98	4.33	2.58	3.90
	Moisture (%)	8.96	8.54	5.73	8.97
	Bulk density (Kg/m ³)	550	680	580	420
	pH	7.67	10.84	1.82	1.55
	pH _{ZC}	7.90	10.20	< 0	< 0
	Conductivity (µS/cm)	44.60	273.10	713	1125
	Iodine number (mg/g)	890.1	201.72	60.62	10.40
	methylene blue number (mg/g)	-	655.20	-	1479.98
Surface area (m ² .g ⁻¹)	S _{acetic acid}	1631.34	625.83	476.86	395.68
	S _{methylene blue}	250.91	663.92	333.37	930.04
	a ₀ (mmol.g ⁻¹)	2.05	0.48	0.92	4.67
	a _s (mmol.g ⁻¹)	6.10	4.50	14.92	11.43
D ₀ (J.m ⁻²)	D ₀ (acetic acid)	4.30	9.27	14.78	7.75
	D ₀ (methylene blue)	27.94	8.74	21.14	3.30
Surface chemistry	Phenolic functions (méq.g ⁻¹)	0.21	0.03	0.63	0.62
	Carboxylic functions (méq.g ⁻¹)	0.06	0.01	0.38	0.35
	Lactones functions (méq.g ⁻¹)	0.04	0.00	0.03	0.08
	Carbonyl functions (méq.g ⁻¹)	-	-	-	-
	Total acid function (méq.g ⁻¹)	0.31	0.04	1.04	1.05
	Total basic function (méq.g ⁻¹)	0.70	0.64	-	-

The different surface areas of these carbons are in agreement with their different iodine and methylene blue numbers. These results confirm the predominance of CAPH1 and CAF1 pores by mini micropores, and those of CAPH2 and CAF2 by average micropores. With regard to values of S_{acetic acid}, CAPH1 has a very high acuity to clean up micropollutants in aqueous solutions such as CAF1 (Gueye *et al.*, 2011). The same is true for CAF2, which has a high capacity to decontaminate macropollutants in aqueous solutions if it is referred to its value of S_{methylene blue} (Gueye *et al.*, 2011; Sakr *et al.*, 2016). The observation of trace values concerning methylene blue numbers for CAPH1 and CAF1 could be explained by their low contact time with this dye during the determination of this index. As a result, the diffusion of this molecule would seem slow in these carbons. Also, different values of surface areas relative to acetic acid and methylene blue of CAPH2 show that this activated carbon has practically the same number of mini micropores and average micropores. Except CAF1, CAPH1, CAPH2 and CAF2 are more efficient than some activated carbons developed in the context of aqueous solutions depollution. For illustration, iodine number and S_{acetic acid} of CAPH1, obtained by chemical activation by ZnCl₂, is greater than that of Yuliusman *et al.* (2017), obtained by activation of kernel shells of *Elaeis guineensis* drupe with KOH and in the same temperature range (648 mg/g for the iodine number and 743 m²/g for surface area (S_{BET})). Also, this carbon has a good capacity compared to that of Babayemi (2017), obtained by activation of the same precursor by H₃PO₄ (iodine number of 558.06 mg/g and surface area of 635.73 m²/g). As for CAPH2, it has more acuity than some carbons, such as that obtained by Bamba *et al.* (2009), obtained by chemical activation of coconut shells by KOH (S_{BET max} = 665.79 m²/g). As regards CAF2, it has a high aptitude compared to other activated carbons based on materials with low lignocellulosic compositions, such as that obtained by Nwabanne and Igbokwe (2011) from

kernels of Nipa palm seed (S_{BET} = 871.22 m²/g) and Chen (2016) from kernels of pine fruit (S_{BET} = 1057.8 m²/g).

CAPH1 and CAPH2 have functional surface groups of basic character. This basic character of these two carbons would be partly due to the free oxygen of basic Lewis sites, often attributed to electrons of graphitic planes (Daoud and Benturki, 2014). It also comes from the presence of some bases such as CaO, Na₂O, MgO (Baudu *et al.*, 2001) and especially K₂O for CAPH2, activated by KOH. This would explain the more pronounced basic and conductive characters of CAPH2 compared to those of CAPH1. pH_{ZC} of CAPH1, very slightly basic, shows that it would behave like an amphoteric (Daoud and Benturki, 2014). This fact is attributed to its activation by ZnCl₂. As for CAPH2, its high value of pH_{ZC} is linked to its activation by KOH (Ruiz *et al.*, 2015). CAF1 and CAF2 have functional surface groups of a completely acidic character, essentially due to phenolic functions. This fact is in accord with their pH value, also influenced by the nature and chemical composition of *Dacryodes klaineana*. Indeed, this precursor whose composition is very close to *Dacryodes edulis* (Ebana *et al.*, 2017), would have a high relative content of HCN, oxalates, phytate, proteins, carbohydrates and fats. Therefore, the activation of this precursor by H₃PO₄ and KOH would have the effect of causing a strong presence of mineral acid compounds in these carbons. This phenomenon would justify their strong relative conductivities, especially CAF2 activated by KOH. Their value of pH_{ZC}, consecutive to this fact, show that these carbons are negatively charged whatever pH considered. Thus, they have great acuity in cationic compounds depollution. Moreover, the total absence of basic functions on these carbons would have its origin by not being in contact during their synthesis with oxygen below 200°C or above 700°C on the one hand, and the absence of their treatment with hydrogen and degassing at room temperature, because it is at this stage that the basic functions are introduced (Maazou *et al.*, 2017), on the other.

Whatever the method used for the determination of their surface area, CAPH1 and CAPH2 are hydrophobic because their surface areas were between 400 and 2500 $m^2 \cdot g^{-1}$ (Weber and Quicker, 2018). For carbons based on kernels of *Dacryodes klaineana* fruit, their hydrophobicity depends on the method used to characterize their surface area. Indeed, CAF1 is hydrophobic taking into account its $S_{acetic\ acid}$, but hydrophilic if it takes into account its $S_{methylene\ bleu}$, while for CAF2 the opposite is noted. This contradiction observed is explained by the ability of kernels of *Dacryodes klaineana* fruit to form more average micropores under conditions used in this study.

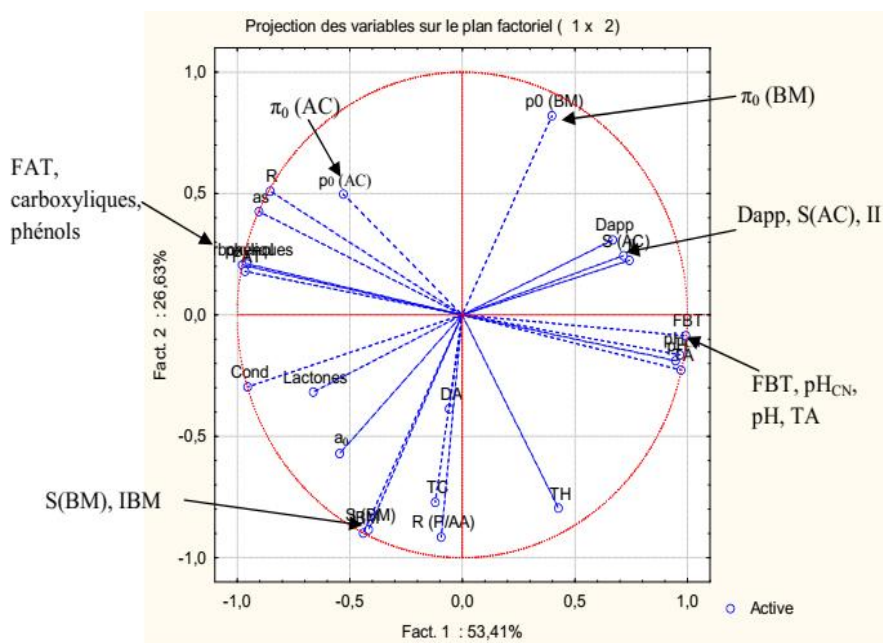
CAF2 have the greatest number of primary polar sites that can give rise to local adsorption with a polar molecule, particularly with water. It is followed by CAPH1. Thus, these two activated carbons have a reactive surface with respect to small polar molecules (Baudu *et al.*, 2001). This fact is more due to the bulk density of these carbons, because this parameter evolves contrary to a_0 with reference to data in Table 4. Activated carbons based on kernels of *Dacryodes klaineana* fruit absorb a quantity of water (as) more important as those obtained from kernel shells of *Elaeis guineensis* drupe. This characteristic is explained by the difference in their texture. Indeed, a powdered activated carbon has a large external surface and a low diffusion depth which generates a very fast adsorption rate on the surface. The granular form of carbons is characterized by a large internal surface and a relatively small external surface, leading to a great deal of diffusion phenomena inside pores in the adsorption process (Yahiaoui, 2012). With reference to molecules of the acetic acid size (mini micropores), CAPH1 has the

most hydrophobic character followed by CAF2. As for the reference taken for polar molecules of the methylene blue size (average micropores), CAF2 is the most hydrophobic followed by CAPH2. These results support the explanation of results obtained in the determination of iodine and methylene blue numbers. The contradiction observed in the case of a_0 (acetic acid), namely between CAF1 and CAF2, is explained essentially by the greatest capacity of CAF1 absorbed water in this study.

Some physical and chemical parameters modeling

Study of different correlations

The first two factors of NPCA express to 82.07% the information due to characteristics activated carbons, including factors used for their synthesis. This result confirms the relevance of initial factors chosen for their synthesis on the one hand, and their good physical and chemical characterization on the other. The first eigenvalue of 11.30 is associated with F1, while the second, of 5.08, is at F2. a_0 ($r = -0.56$), a_s ($r = -0.90$), yield ($r = -0.84$), bulk density ($r = 0.68$), pH ($r = 0.95$), pH_{ZC} ($r = 0.97$), conductivity ($r = -0.96$), iodine number ($r = 0.74$), $S_{acetic\ acid}$ ($r = 0.72$), phenolic functions ($r = -0.95$), carboxylic functions ($r = 0.97$), lactones functions ($r = -0.67$), total acid function ($r = -0.96$), total basic function ($r = 0.99$) have a strong correlation with F1. It is the same for all activated carbons synthesized with F1. A strong correlation of a_0 ($r = -0.57$), a_s (methylene blue) ($r = 0.82$), ash ($r = -0.77$), moisture ($r = -0.80$), methylene blue number ($r = -0.90$), $S_{methylene\ blue}$ ($r = -0.88$), impregnation rate ($r = -0.92$) are noted with F2 (Fig. 2A). CAF1 and CAF2 have a strong correlation with F2 (Fig. 2B).



A

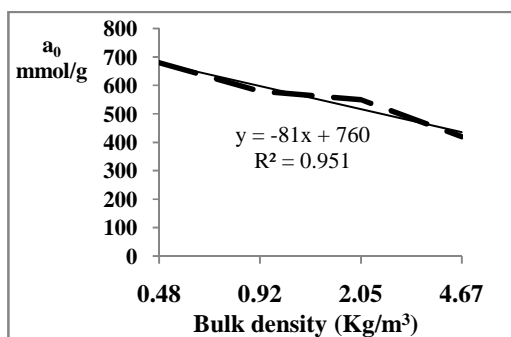
acetic acid)) ($r' = -0.98$) respectively for all activated carbons. The strong correlations observed between the iodine number and $S_{\text{acetic acid}}$ ($r' = 1.00$), and between the methylene blue number and $S_{\text{methylene blue}}$ ($r' = 0.98$) confirm the relevance of iodine and methylene blue as probe molecules for the evaluation of surface areas of these activated carbons. There is a strong correlation between pH and pH_{ZC} , which evolve identically ($r' = 1.00$) for all activated carbons. These two parameters are influenced by surface functions of these carbons with which they have same correlation values. For CAF1 and CAF2, the drop in their pH and pH_{ZC} are mainly due to a relatively strong presence of phenolic functions ($r' = -1.00$), carboxylic functions ($r' = -1.00$), therefore of the total acid function ($r' = -1.00$) where they are in the majority. A particularity is observed for pH_{ZC} which linearly increases with the total basicity of these carbons ($r' = 1.00$) and with their activation temperature ($r' = 1.00$). Most of CAF1 and CAF2 surfaces acidity due mainly to phenolic and carboxyl functions is illustrated by the strong correlation between these parameters ($r' = 1.00$). Naturally, it follows from their absence on CAPH1 and CAPH2, translated by a correlation of these organic functions with the basic total function, of -1.00 . This is also confirmed by the observation for all these carbons of the totally opposite evolution of the total acid function with the total basic function ($r' = -1.00$), phenolic and carboxyl functions with the total basic function, respectively of -0.95 and -0.98 . The important effect of the activation temperature on the development of surface functions (Chauvin 2015, Meljac 2014) is further confirmed by the different correlations obtained during this study. The high activation temperatures for obtaining CAPH1 and CAPH2 favored a development of basic functions on the surface of these carbons, unlike CAF1 and CAF2 activated at relatively

low temperatures. This is confirmed by the correlation value of -0.96 between phenolic functions and activation temperature, of -0.99 between carboxyl functions and activation temperature, of -1.00 between the total acid function and activation temperature, of -1.00 between the total basic function and activation temperature. The ash of all carbons generally increases with the impregnation rate ($r' = 0.96$).

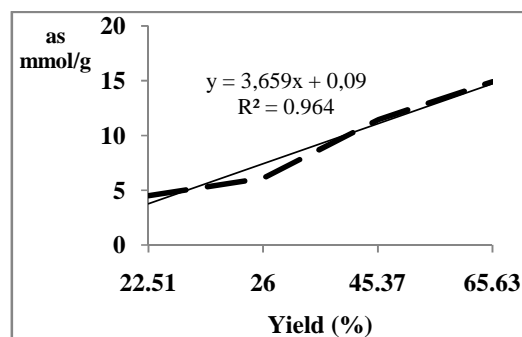
Modeling by simple linear regression

The NPCA and non-parametric coefficients of Spearman have shown that all physical and chemical characteristics of these carbons are strongly correlated directly and/or indirectly. Thus, simple linear correlations can be used to model each according to the others. In the interest of easy prediction of some of these parameters, it seems more judicious to establish models from easily determinable parameters such as the yield, the activation temperature and the bulk density, which is relatively easy to obtain.

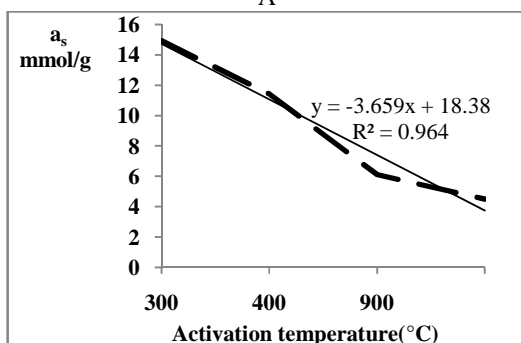
By operating under conditions for obtaining optimal carbons in accordance with the microporosity from precursors used in this study, a_0 and lactones functions of an active carbon obtained are determined at 95.10% and 94.40% from the bulk density (Fig. 3A and 3E). It is the same for a_s estimated at 96.40% from the yield of these carbons (Fig. 3B). Again, in same conditions, except the activation temperature, a_s and the yield is estimated to be close to 96.40% and 93.10% from the activation temperature respectively (Fig. 3C and 3D). On the same basis, pH_{ZC} , phenolic functions, the total acid function and the total basic function are estimated at 87.10% (Fig. 4A), 92.25% (Fig. 4B), 88.60% (Fig. 4C), 88.10% (Fig. 4D) and 83.20% (Fig. 4E) respectively from the activation temperature.



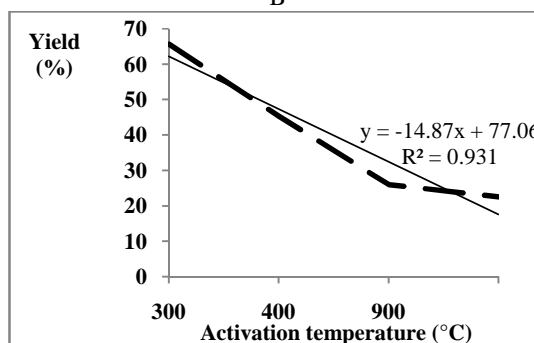
A



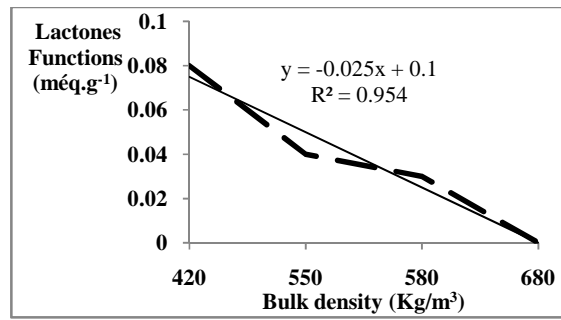
B



C

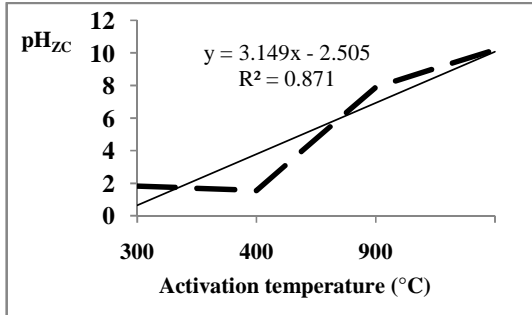


D

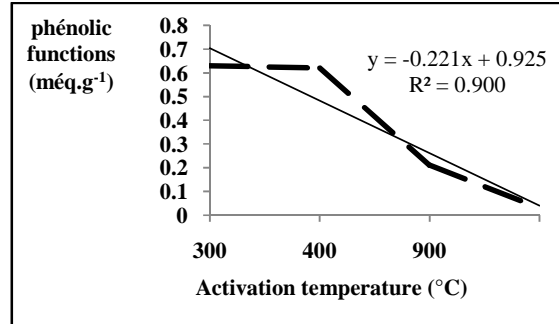


E

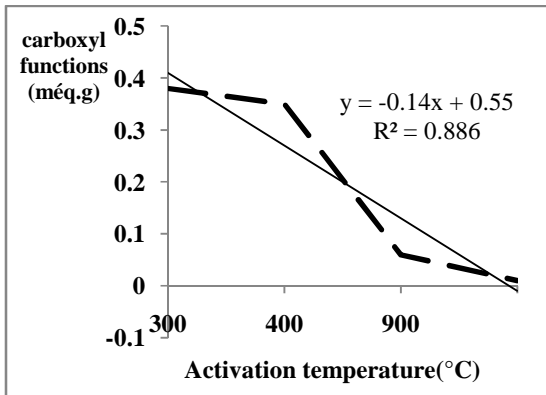
FIGURE 3: Linear relationship between a_s and the bulk density (A), a_s and the yield (B), a_s and the activation temperature (C), the yield and the activation temperature (D), lactones functions and the bulk density (E).



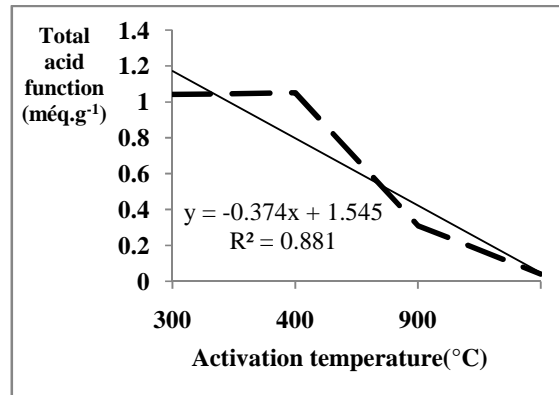
A



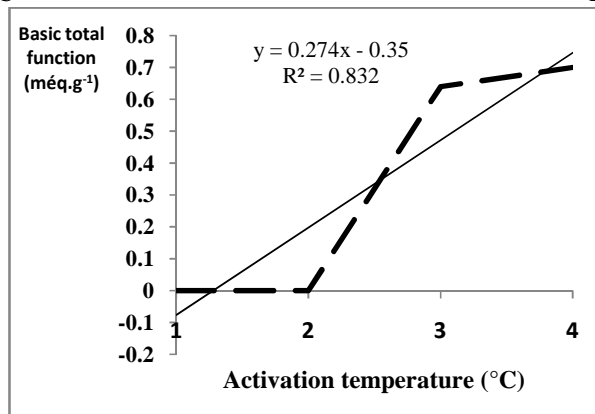
B



C



D



E

FIGURE 4: Linear relationship between pH_{ZC} and the activation temperature (A), phenolic functions and the activation temperature (B), carboxyl functions and the activation temperature (C), the total acid function and the activation temperature (D), the total basic function and the activation temperature (E).

CONCLUSION

This study showed the acuity of 2^k full factorial design for activated carbons synthesis. It showed again the good capacity of precursors used to obtain activated carbons of good qualities, except for kernels of *Dacryodes klaineana* fruit in the case of an activated carbon containing maximum mini micropores in experimental conditions used. This observation is illustrated by the relative importance of their surface area, iodine and methylene blue numbers according to the microporosity considered. Also, with relatively high yields achieved at activation temperatures used, these carbons have low ash and moisture. These physical and chemical characteristics indicate their superior quality favoring adsorption, as well as their high calorific value. Also their low bulk densities testify to their important volume of activity, punctuated by their optimal quality. Activated carbons based on kernel shells of *Elaeis guineensis* drupe have a granular texture and are all basic. Those based on kernels of *Dacryodes klaineana* fruit are powdery and acidic. The activated carbon based on kernel shells of *Elaeis guineensis* drupe, obtained by activation with $ZnCl_2$, has a good capacity for micropollutants depollution. It could therefore be used for the drinking water depollution. The one based on this same precursor and obtained by activation with KOH have both the pollution abatement capabilities of micropollutants and macropollutants. This carbon could be used for both drinking water and dyes depollution in aqueous solutions. The carbon derived from kernels of *Dacryodes klaineana* and activated by KOH can only be used for macropollutants depollution such as dyes in aqueous solutions. These results once again confirm the high capacity of kernel shells of *Elaeis guineensis* drupe for the production of activated carbons and its use in the fight against environmental pollution. They also allowed to the reevaluation of kernels of *Dacryodes klaineana* fruit as a precursor potential for the production of activated carbons. This work deserves to be complemented by other studies aimed at improving it further. For this purpose, the experimental study of synthetic or real solutions depollution by these activated carbons should be considered. These carbons could also be used by coupling with other techniques in the fight against environmental pollution. Also, would it be possible to use 2^k full factorial design for activated carbons synthesis based on these precursors by the physical activation, in order to verify the effect of this method on their physical and chemical properties compared to those obtained in this study. This experimental design could also be applied to other low-yielding plant biomasses that abound in the Ivorian environment for the production of activated carbons, and to compare results with those already obtained in this study.

ACKNOWLEDGEMENTS

Authors wishes to express his appreciation to Dr. BAMBA Siaka Barthelemy, Director of Oceanologic Research Center of Abidjan.

REFERENCES

Andas, J., Rahman, M.L.A. and Yahya, M.S.M. (2017) Preparation and Characterization of Activated Carbon

from Palm Kernel Shell. IOP Conf. Ser., Mater. Sci. Eng. 226 012156

ASTM D2854-09 (2014) Standard Test Method for Apparent Density of Activated Carbon.

ASTM D 2867- 09 (2014) Standard Test Methods for Moisture in Activated Carbon.

ASTM D3174-12 (2012) Standard Test Method for Ash in the Analysis Sample of Coal and Coke from Coal.

ASTM D 3838-80 (1999) Standard Test Method for pH of Activated Carbon.

ASTM D4607-94 (2011) Standard Test Method for Determination of Iodine Number of Activated Carbon.

Avom, J., Mbadcam, J.K., Matip, M.R.L. and Germain, P. (2000) Adsorption isotherme de l'acide acétique par des charbons actifs d'origine végétale. Afri. J. Sci. Technol., Sci. Eng. Ser. 2 (2), 1-7.

Babayemi, A.K. (2017) Performance Evaluation of Palm Kernel Shell Adsorbents for the Removal of Phosphorus from Wastewater. Adv. Chem. Eng. Sci. 7, 215-227.

Bamba, D., Dongui, B., Trokourey, A., Zoro, G.E., Athéba, G.P., Robert, D. and Wéber, J.V. (2009) Études comparées des méthodes de préparation du charbon actif, suivies d'un test de dépollution d'une eau contaminée au diuron. J. Soc. Ouest-Afr. Chim. 28, 41-52.

Baudu, M., Guibaud, G., Raveau, D. and Lafrance, P. (2001) Prévision de l'adsorption de molécules organiques en solution aqueuse en fonction de quelques caractéristiques physico-chimiques de charbons actifs. Water Qual. Res. J. Can. 36(4), 631-657.

Boehm, H.P. (1966) Chemical identification of surface groups, in Advances in catalysis. Eley D.D., Pines H., Weisz (éd.), 16, pp. 179-274, Academic Press, New York.

Cao, L., Yu, I.K.M., Tsang, D.C.W., Zhang, S., Ok, Y.S., Kwon, E.E., Song, H. and Poon, C.S. (2018) Phosphoric acid-activated wood biochar for catalytic conversion of starch-rich food waste into glucose and 5-hydroxymethylfurfural. Bioresour. Technol. 267, 242-248.

Chauvin, E. T. (2015) Préparation de charbon actif à partir de coques de noix de palmier à huile pour la récupération d'or et le traitement d'effluents cyanurés. Thèse de l'université catholique de Louvain, France.

Chen, D., Chen, X., Sun, J., Zheng, Z. and Fu, K. (2016) Pyrolysis polygeneration of pine nut shell: Quality of pyrolysis products and study on the preparation of activated carbon from biochar. Bioresour. Technol., 216, 629-636.

ECCMF, (1986) Blue methylene value. In Test Methods for activated carbon, CEFIC (eds), pp.25-27, Europe.

- Daoud, M. and Benturki, O. (2014) Activation d'un charbon à base de noyaux de jujubes et application à l'environnement. Adsorption d'un colorant de textile. Rev. Énerg. Renouvelables SIENR'14 Ghardaïa, 155-162.
- Ebana, R.U.B., Edet, U.O., Ekanemesang, U.M., Ikon, G. M., Umoren, E.B., Ntukidem, N.W., Etim, O.E., Sambo, S. and Brown, N.U. (2017) Proximate Composition and Nutritional Analysis of Seeds and Testas of *Dacryodes edulis* and *Garcinia kola*. Asian J. Biol. 2(1), 1-8.
- Ello, A.M., De Souza, L. K.C., Trokourey, A. and Jaroniec, M. (2013) Development of microporous carbons for CO₂ capture by KOH activation of African palm shells. J. CO₂ Utilization 2, 35-38.
- Elmouwahidi, A., Bailón-García, E., Pérez-Cadenas; A.F., Maldonado-Hódar, F. J. and Carrasco-Marín, F. (2017) Activated carbons from KOH and H₃PO₄-activation of olive residues and its application as super capacitor electrodes. Electrochimica Acta 229 (1), 219-228.
- GIZ (2013) Étude sur l'exploitation forestière et les contraintes d'une gestion durable des forêts dans le domaine rural en Côte d'Ivoire. CIRAD, France.
- Gnagne, Y.A., Yapo, B.O., Meité, L., Kouamé, V.K., Gadji, A.A., Mambo, V. and Houenou P. (2015) Caractérisation physico-chimique et bactériologique des eaux usées brutes du réseau d'égout de la ville d'Abidjan. Int. J. Biol. Chem. Sci. 9(2), 1082-1093.
- Gnonsoro, U.P., Yao, K.M., Yao, B.L., Kouassi, A.M., Dembélé, A., Kouakou, Y. U., Ouatarra, K. P. H., Diabaté, D. and Trokourey, A. (2015) Adsorption du benzo(a)pyrène sur du charbon activé à base de coques de coco provenant de Côte d'Ivoire. Int. J. Biol. Chem. Sci. 9(5), 2701-2711.
- González-García, P., 2018. Activated carbon from lignocellulosics precursors: A review of the synthesis methods, characterization techniques and applications. Renew. Sustain. Eng. Rev. 82(1), 1393-1414.
- Guety, T. P., Koné, B., Yao, G. F., Kouakou, Y. N. and Yao-Kouamé, A. (2015) Concentrations of copper, lead and zinc in soils and vegetables organs from periurban agriculture areas of Abidjan Côte d'Ivoire. J. Agric. Ecol. Res. Int. 3 (1), 12-23.
- Gueye, M., Blin, J. and Brunschwig, C., (2011) Étude de la synthèse des charbons actifs à partir de biomasses locales par activation chimique avec H₃PO₄. 6ème journées scientifiques du 2iE, Campus 2iE Ouagadougou, Burkina Faso. 4-8 Avril 2011.
- Hidayua, A.R and Mudaa, N. (2016) Preparation and characterization of impregnated activated carbon from palm kernel shell and coconut shell for CO₂ capture. Procedia Eng. 148, 106-113.
- Igwegbe, C. A., Onyechi, P. C. and Onukwuli, O. D., (2015) Kinetic, Isotherm and Thermodynamic Modelling on the Adsorptive Removal of Malachite Green on *Dacryodes edulis* Seeds. J. Sci. Eng. Res. 2(2), 23-39.
- Julien, F, Baudu, M, and Mazet, M. (1998) Relationship between chemical and physical surface properties of activated carbon. Water Res. 32, 3414–3424.
- Kouakou, Y.U., Essy, K.F., Dembélé, A., Brou, Y.S., Ello, S.A., Gouli Bi, I.M. and Trokourey, A. (2017) Removal of imidacloprid using activated carbon produced from *Ricinodendron heudelotii* shells. Bull. Chem. Soc. Ethiop. 31(3), 397-409.
- Kouotou, D., Manga, H.N., Baçaoui, A., Yaacoubi, A. and Mbadcam, J.K. (2013) Optimization of activated carbons prepared by and steam activation of oil palm shells. J. Chem. 2013, 1-10.
- Lopez-Ramon, M.V., Stoeckli, F., Moreno-Castilla, C. and Carrasco-Marín, F. (1999) On the characterization of acidic and basic surface sites on carbons by various techniques. Carbon 37, 1215-1221.
- Maazou, S.D.B., Hima, H.I., Malam, A.M.M., Adamou, A. and Natatou, I. (2017) Élimination du chrome par du charbon actif élaboré et caractérisé à partir de la coque du noyau de *Balanites Aegyptiaca*. Int. J. Biol. Chem. Sci. 11(6), 3050-3065.
- Marouane, S., Saile, R. and El Kettani, M. A. E-C. (2016) Les outils qualité au service de la recherche: L'optimisation du procédé de valorisation de la biomasse par les plans d'expériences. J. Mater. Environ. Sci. 7 (1), 105-112.
- Mbaye, G. (2014) Développement de charbon actif à partir de biomasse lignocellulosique pour des applications dans le traitement de l'eau. Thèse de doctorat en technologie de l'Eau, de l'Energie et de l'Environnement. 2iE, Burkina Faso.
- Meljac, L. (2004) Étude d'un procédé d'imprégnation de fibres de carbone activées. Thèse de l'École Nationale Supérieure des Mines de Saint-Etienne, France.
- N'Gotta, C. (2009) Évaluation de la qualité de l'air à Abidjan: Une approche par la méthode de l'évaluation contingente. Master NPTCI, Université de Cocody-Abidjan, Côte d'Ivoire.
- N'Guessan, Y.A., Wango, T-E, Konan, K. E., Adingra, A., Amani, E. M., Monde, S., Affian K. and Aka, K. (2015) Hydrologie et morphologie de l'estuaire du fleuve Sassandra, Basse Côte d'Ivoire. Afr. Sci. 11(2), 161-172.
- Nunes, C.A. and Guerreiro, M.C. (2011) Estimation of surface area and pore volume of activated carbons by methylene blue and iodine numbers. Quím. Nova 34(3), 472-476.
- Nwabanne, J.T. and Igbokwe, P.K. (2011) Preparation of activated carbon from Nipa palm nut: influence of preparation conditions. Res. J. Chem. Sci. 1(6), 53-58.

- Okoroigwe, E.C., Ofomatah, A.C., Oparaku, N.F. and Unachukwu, G.O. (2013) Production and evaluation of activated carbon from palm kernel shells (PKS) for economic and environmental sustainability. *Int. J. Phy. Sci.* 8(19), 1036-1041.
- Olowoyo, D.N. and Orere, E.E. (2012) Preparation and Characterization of Activated Carbon Made From Palm-Kernel Shell, Coconut Shell, Groundnut Shell and *Obeche* Wood (Investigation of Apparent Density, Total Ash Content, Moisture Content, Particle Size Distribution Parameters). *Int. J. Res. Chem. Environ.* 2(3), 32-35.
- Ousmaila, S.M., Adamou, Z., Ibrahim, D. and Ibrahim, N. (2016) Préparation et caractérisation de charbons actifs à base de coques de noyaux de *Balanites Eagyptiaca* et de *Zizyphus Mauritiana*. *J. Soc. Ouest-Afr. Chim.* 41, 59-67.
- Ruiz, H., Zambrano, M., Giraldo, L., Sierra, R. and Moreno-Pirajan, J.C. (2015) Production and characterization of activated carbon from oil-palm shell for carboxylic acid adsorption. *Orient. J. Chem.* 31(2), 753-762.
- Sakr, F., Sennaoui, A., Elouardi, M., Tamimi, M. and Assabbane, A. (2015) Étude de l'adsorption du Bleu de Méthylène sur un biomatériau à base de Cactus (Adsorption study of Methylene Blue on biomaterial using cactus). *J. Mater. Environ. Sci.* 6 (2) 397-406.
- Sethupathi, S., Bashir, M.J.K., Akbar, Z.A. and Mohamed, A.R. (2015) Biomass-based palm shell activated carbon and palm shell carbon molecular sieve as gas separation adsorbents. *Waste Manag. Res.* 33(4) 303-312.
- Siragi, D.B., Maazou, S.D.B., Halidou, I.H., Malam A.M. M., Zanguina, S.Y. and Fu, Y. (2018) KOH-activated rice husk char via CO₂ pyrolysis for phenol adsorption. *Mater. Today Eng.* 9, 397-405.
- Shen Y. and Fu Y. (2018) KOH-activated rice husk char via CO₂ pyrolysis for phenol adsorption. *Mater. Today Eng.* 9, 397-405.
- Shoemaker, D.P., Garlang, C.W., Steinfeld, J.I. and Nibler J.W. (1981) Experiments in physical chemistry. 4th eds, MC Graw-Hill Book Co, New-York.
- Wahyuningsih, Z.A., Mohamad, E.Y., Indah, H. and Eflita, Y. (2018) Preparation and characterization of oil palm shell activated carbon by alkali chemical activation method. *AIP Conference Proceedings* 1977, 020028 (2018). Conference: human-dedicated sustainable product and process design: Materials, resources, and energy: Proceedings of the 4th International Conference on Engineering, Technology, and Industrial Application (ICETIA) 2017.
- Weber K., Quicker P., 2018. Properties of biochar. *Fuel*, 217, 240-261.
- World Bank (2017) United Nations Population Division. World Population Prospects: 2017, Revision. <https://data.worldbank.org/indicator/SP.DYN.LE00.IN>
- Xia, D., Tan, F., Zhang, C., Jiang, X., Chen, Z., Li, H., Zheng, Y., Li, Q. and Wang, Y. (2016) ZnCl₂-activated biochar from biogas residue facilitates aqueous As(III) removal. *Appl. Surf. Sci.* 377, 361-369.
- Yahiaoui, N. (2012) Étude de l'adsorption des composés phénoliques des margines d'olive sur carbonate de calcium, hydroxyapatite et charbon actif, Mémoire de Magister, Université de Tizi Ouzou, Algérie.
- Yuliusman, N., Afdhol, M.K., Amiliana, R.A. and Hanafi, A. (2017) Preparation of activated carbon from palm shells using KOH and ZnCl₂ as the activating agent. *IOP Conf. Series: Earth and Environ. Sci.* 75 (2017) 012009.
- Zeroual, S., Guerfi, K., Hazourli, S. and Charnay, C. (2011) Estimation de l'hétérogénéité d'un charbon actif oxydé à différentes températures à partir de l'adsorption des molécules sondes. *Rev. Énerg. Renouv.* 14(4), 581-590.